Geophysical Research Letters

RESEARCH LETTER
10.1029/2021GL094265

Atmospheric Rivers and Snow Accumulation in the Upper Colorado River Basin

Mu Xiao[1,2] **and Dennis P. Lettenmaier**[1]

[1]Department of Geography, University of California, Los Angeles, CA, USA, [2]Now at School of Sustainable Engineering and the Built Environment, Arizona State University, Tempe, AZ, USA

Key Points:

- Atmospheric river (AR) induced snow accumulation accounts for 30.8% of the peak snow water equivalent in the Upper Colorado River basin (UCRB)
- Most of the ARs that reach the UCRB first intercept the Sierra Nevada Region
- Aside from very dry conditions, the AR contribution to UCRB snowpack during warm winters is greater than average

Supporting Information:

Supporting Information may be found in the online version of this article.

Correspondence to:

D. P. Lettenmaier,
dlettenm@ucla.edu

Citation:

Xiao, M., & Lettenmaier, D. P. (2021). Atmospheric rivers and snow accumulation in the Upper Colorado River basin. *Geophysical Research Letters*, *48*, e2021GL094265. https://doi.org/10.1029/2021GL094265

Received 9 MAY 2021
Accepted 24 JUL 2021

Abstract We utilized a macroscale hydrology model in conjunction with an atmospheric river (AR) catalog to evaluate AR-affected snow accumulation in the Upper Colorado River basin (UCRB) headwaters for water years 1951–2015. We find that there are on average 11.4 days during which AR-originating snow accumulates in the UCRB each year, yielding 5.75 km^3 of snow water equivalent (SWE). This AR-originating SWE accounts for 30.8% of average annual peak SWE in the basin. Most of the ARs that reach the UCRB first intercept the Sierra Nevada region of California; 84% of days affected by ARs in the UCRB are also AR-affected days in the Sierra Nevada. The pathways of the ARs reaching the UCRB do not have a great effect on snow accumulation, however ARs that first pass through the Sierra Nevada generally produce greater snow accumulations there than in the UCRB.

Plain Language Summary Atmospheric rivers (AR), commonly defined as corridors of concentrated water vapor in the atmosphere, can yield large amounts of snow accumulation when they make landfall during the cold season. As over half of the naturalized streamflow in the Colorado River originates from water released by snow melt, it is of great significance to understand how atmospheric rivers can affect the snowpack in the basin. Here, we identify the atmospheric rivers in the Upper Colorado River basin during a 65-years-long historical record and evaluate their contribution to mountain snowpack. Almost one third of snowpack in the basin is attributed to atmospheric river induced snowfall. The primary origin of the relevant ARs is from the southwest, although the ARs' pathways do not much affect the amount of snow they yield. Non-AR-related snowfall is highly important to the basin's snow accumulation during cold years, while AR contributions to snow are greater under warm conditions.

1. Introduction

The Colorado River is the largest river in the U.S. Southwest, and the region's most important surface water source. The area of the entire Colorado River basin is ~637,000 km^2, and more than 90% of its streamflow is generated in the Upper Colorado Basin (UCRB) above Lees Ferry, AZ. It is one of the most heavily regulated rivers in the world, owing to municipal and agricultural water demands in the Lower Basin (below Lees Ferry) where some 13,000 km^2 of agricultural lands are irrigated with river water (Cohen et al., 2013). The river's natural flow is highly influenced by snowpack in the Rocky Mountain headwaters subbasins, which account for over 70% of the river's annual streamflow (Li et al., 2017). As atmospheric rivers (AR), commonly defined as narrow corridors of atmospheric water vapor (Neiman et al., 2008), can lead to extreme precipitation when making landfall in the mountainous regions (Eldardiry et al., 2019), they should have nonnegligible impact on water resources in the UCRB. Given the exceptionally high use of the river's water and the need to efficiently manage it in the face of a warming climate, better understanding of the hydrological behavior and patterns within the basin are of great interest both to the scientific and water management communities.

It is now understood that ARs contribute 30%–70% of seasonal maximum accumulated snow water equivalent (SWE) in the Sierra Nevada (SN; Dettinger, 2016; Eldardiry et al., 2019; Huning et al., 2019). During large-scale AR-related events, atmospheric moisture is forced to raise and cool when crossing topographic barriers, yielding large amounts of winter snowfall in the mountain headwaters. However, equivalent statistics are not available for the UCRB, despite the significance of the snowpack in the UCRB headwaters to the growing population centers of the Southwest. Given the fact that both frequency and intensity of AR events are lower in UCRB compared to those along the west coast (Albano et al., 2020; Ralph et al., 2019;

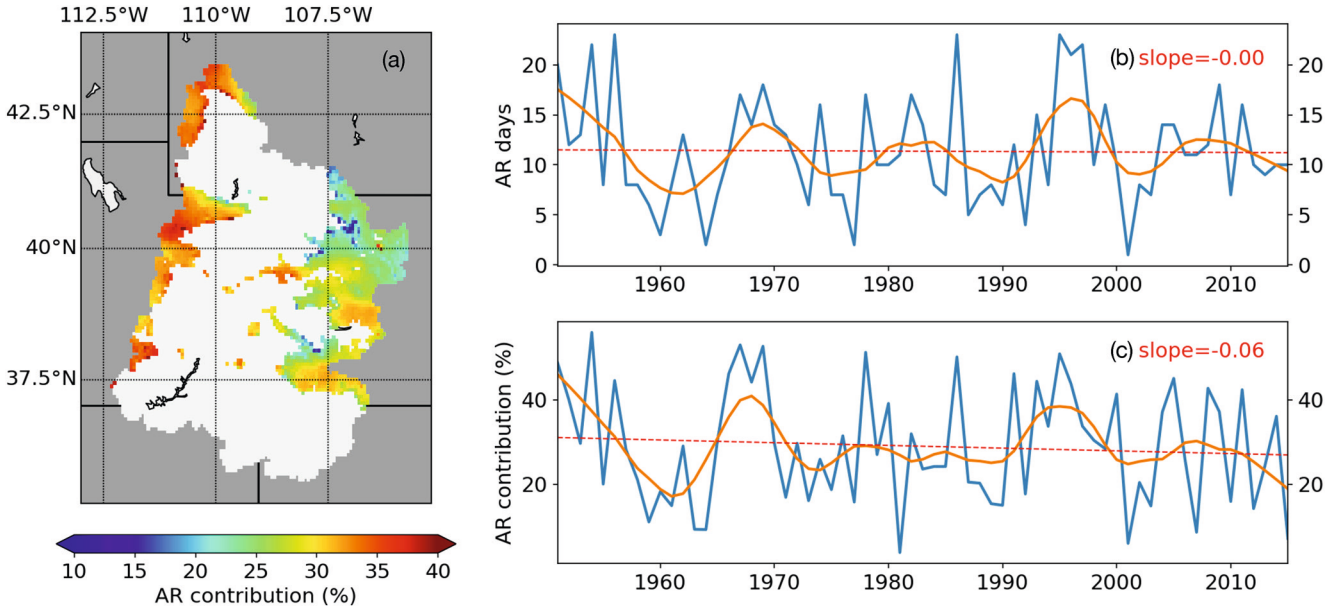

Figure 1. (a) Average atmospheric river (AR) snowpack contribution (per winter) as percentage of total snowpack accumulation across all the 1/16° grid cells with long-term average Variable infiltration capacity snow water equivalent (VIC SWE) on April 1 >50 mm in the study domain. (b) Annual time series of valid AR days in the Upper Colorado River basin (UCRB) for 1951–2015. The red dashed line is the linear regression against time (not statistically significant). The orange line is smoothed using a LOWESS fitter with fraction = 0.17. (c) Same as panel (b) but for the fraction of total snow accumulation attributable to ARs (regression not statistically significant).

Shields et al., 2018; Swales et al., 2016), the effects of ARs on hydroclimate in the UCRB are expected to be less significant than in the Sierra Nevada.

Although an analysis to identify the long-term contribution of ARs to snow accumulation in the UCRB has not previously been undertaken, several earlier studies are relevant. Utilizing ERA-Interim reanalysis AR and in situ measurements over 1998–2008, Rutz and Steenburgh (2012) reported that winter precipitation in the interior of the western United States is less affected by AR events compared to the coastal areas—AR contribution to winter precipitation in California is usually twice that in the interior of the West. Kirk and Schmidlin (2018) identified two main trajectories of UCRB's large precipitation events associated with atmospheric rivers: flow from the southwest coast mainly contributing to UCRB's southern region and flow from the west advecting moisture to UCRB's northern region. Huning et al. (2019) compared four atmospheric reanalysis data sets for AR detection in the Sierra Nevada and found that snowfall attribution to ARs can be sensitive to horizontal resolution.

Here, we utilize a physically based, semidistributed hydrological model to simulate SWE over the headwaters of the UCRB (Figure 1a) for water years (October 1 to September 30) 1951–2015 (hereafter any reference to years implies water years unless stated otherwise). Then, we determine the snow accumulation attributable to ARs and evaluate the hydrologic characteristics of AR-induced snow in the UCRB. The ARs' effect on snow in the UCRB are further compared to that in the Sierra Nevada mountain region.

2. Data and Methods

2.1. Hydrologic Modeling

We used the variable infiltration capacity (VIC) model (Liang & Lettenmaier, 1994) version 4.2.d as our primary tool to generate SWE records over the UCRB. The snow module in VIC employs a two-layer scheme to represent the snowpack. In addition, canopy interception and solar radiation attenuation effect are considered (Andreadis et al., 2009), which has been successfully applied in a number of previous studies on snow-related hydroclimatology in the UCRB (e.g., Deems et al., 2013; Mote et al., 2005, 2018; Painter et al., 2010). Because we are only interested in snow-related regions in this paper, we defined the study

domain as all 1/16th degree grid cells in the UCRB whose long-term average April 1 SWE (as simulated by the VIC model) exceeded 50 mm (see Figure S1). We implemented the same parameters and set-up of VIC as in Li et al. (2019).

The VIC model requires gridded meteorological forcings; we used daily gridded values of precipitation, temperature maximum and minimum, and wind speed from the extended Livneh data set (Livneh et al., 2015; Su et al., 2021). We applied the Mountain Climate (MTCLIM) algorithms (see Bohn et al., 2013 for details) to produce downward longwave and shortwave radiation, surface air pressure, and humidity from the original forcings and then ran the VIC model with these meteorological inputs. VIC-simulated SWE is reported in mm (as is precipitation).

2.2. Model Verification and AR Catalogs

Simulated VIC snowpack in the California was evaluated by Li et al. (2019), and we used the same approach here, with a focus on UCRB. In particular, we evaluated the model's performance in the UCRB using 86 SNOTEL sites that were screened to assure that all have at least 25 years of usable record during 1981–2015. The average VIC SWE across the 86 SNOTEL stations is generally in good agreement with in situ observations during the accumulation season (Figure S2). Additional details of the performance of the VIC snow simulations relative to SNOTEL observations are provided in Text S1.

The AR catalog we used is the AR database version 1.0 derived by Guan and Waliser (2015). Their catalog was generated using 6-h global atmospheric products at 2.5° spatial resolution from the NCEP-NCAR reanalysis (Kalnay et al., 1996) for calendar years 1950–2015. The main advantage of the Guan and Waliser catalog is its long temporal coverage (some other catalogs have higher spatial resolution but are limited to shorter time periods). Although the spatial resolution of the Guan and Waliser catalog is somewhat coarse, it has been evaluated in comparison with higher resolution catalogs. For instance, Eldardiry et al. (2019) compared the Guan and Waliser catalog to another widely used AR catalog (Neiman et al., 2008) and reported a high percentage of agreement (91%) during the cold season along the west coast.

2.3. AR-Related Snow Identification

To evaluate AR contributions to snowpack, we followed the approach of Huning et al. (2019) to assess snow accumulation based on SWE records. We focused on the winter season, which we defined as November 1–March 31. Basin-wide daily SWE net increases (from the VIC model) during the winter were extracted and summed to provide an estimate of total snow accumulation for each year. All calendar days in the study period were classified into AR and non-AR categories using the Guan and Waliser (2015) catalog. Due to uncertainties in atmospheric river detection, we only flagged AR events that persisted in the UCRB study domain as in Huning et al. (2019). Specifically, we considered an AR derived from the 6-h catalog to be "valid" if it intercepted the domain for at least 18 h in the same day, as in Huning et al. (2019). We then counted snow accumulation in the domain during an extended window (the current date as well as 1 day before and 1 day after) for all valid AR days. If the basin-wide ΔSWE was smaller than 0.008 km^3 (0.1 mm vertically), it was not considered as snow accumulation. Consecutive valid AR days were merged into multiday events and then the extended window was applied (1 day before and after the multiday event). In this way, all days with snowfall were classified into AR-related and non-AR categories. More details and results are provided in Section 3.

2.4. AR Pathway

For each valid AR day identified in Section 2.3, we evaluated the shape of the event (using the Guan and Waliser AR catalog) to determine other affected areas outside UCRB by the same AR. Given a specific valid AR day in UCRB (intercepting the domain for at least 18 h in 1 day), all the 6-h records of that day were first extracted. If other grid cells experienced the same AR event for at least 6 h (one single time step), those cells were considered as belonging to that AR's pathway. Although some gird cells are only intercepted by a UCRB's valid AR for 6 or 12 h, they are still part of the AR. Therefore, we did not require the 18-h threshold be crossed for pixels outside UCRB to assess the pathways. By counting the occurrences of the

corresponding ARs at different grid cells, we obtained information about how areas outside UCRB were affected by ARs that are valid in UCRB.

3. Results and Interpretation

3.1. AR-Related Snow in the UCRB

We applied the methods described in Section 2.3 to identify all days during which a valid AR event intercepted the UCRB for the winters of 1951–2015. After identifying valid AR days, we integrated the domain-wide SWE increases (i.e., $\Delta SWE > 0$) in the extended AR windows to determine AR-related snow accumulation. Over the entire study period, there were on average 11.4 valid AR days per winter (November 1–March 31) in the UCRB. Including window edges (with days before and after valid AR days), there were an average of 26.0 days affected by AR events per winter. Seventy-seven percent of the days within the AR windows (20.1 days per year) yield snow accumulation in the domain. Snow occurring on these days averaged 5.75 km^3 snow increase per winter in the basin, accounting for 30.8% of UCRB's average snow accumulation (18.67 km^3/yr). The remaining 69.2% of snow accumulation in the domain is attributed to ordinary winter precipitation events. Compared to all snowfall days, AR-snowfall days have 68% greater snow increase per day than the average (4.04 mm/day versus 2.40 mm/day). We also conducted a two-sample *t* test and found that the inferred 68% difference was statistically significant at the 0.05 level. Annual time series plots of valid AR days per winter and AR-related snow accumulation percentages in the study domain are shown in Figures 1b and 1c, respectively. The percentage of annual snow accumulation attributed to AR-snowfall ranges from 4% to 56%. Rutz and Steenburgh (2012) reported the percentage of total winter precipitation on the AR days and the day following those days is between 20% and 30% during 1998–2008 in the UCRB's SNOTEL sites. The average percentage of snowfall for 1998–2008 in our results is 27.3% across the study domain, which is consistent with Rutz and Steenburgh (2012). We tested for trend in the time series of AR-related snow accumulation and valid AR days (using both the Theil-Sen slope estimator and linear regression), but neither was statistically significant (p value >> 0.05) using either test.

We also investigated spatial variations in AR contribution to snow accumulation in UCRB on a grid cell by grid cell basis. By dividing the AR-related snow by total accumulated snow in each pixel for all the winters, we calculated the contribution of AR to snowpack at each grid cell. Figure 1a shows the spatial distribution of 1951–2015 average AR contribution to total SWE over the UCRB. The western part of the domain has higher percentages than the eastern part; furthermore, the northeastern part of the basin, where most streamflow in the Colorado River is produced, is less affected by ARs compared to other areas. The spatial patterns of AR contribution are consistent with AR events transitioning the UCRB from west to east, as we discuss further in the next section. In addition to the basin-average AR contribution trend analysis, we also computed the trend at each 1/16°-resolution pixel in the study domain. We applied the Mann-Kendall trend test (Kendall, 1957; Mann, 1945) to detect whether there was a significant trend in March 31 SWE and annual AR contribution to snowpack at every single grid cell. There are ~20% cells showing significant trends in March 31 SWE (4.0% increase and 17.8% decrease), but most cells (<2%) in the basin show no significant trend in the AR contribution.

3.2. Pathways of ARs That Intercept the UCRB

Having identified all the valid UCRB AR events, we tracked down each AR's affected pixels and counted AR occurrences at each pixel. Figure 2a shows the frequency of UCRB AR occurrence at all 2.5° grid cells over the Western United States (both inside and outside the UCRB). Red dots (105.0°–112.5°W) mark the region where the ARs were considered to have intercepted the UCRB. Figure 2a shows that the UCRB ARs most frequently also crossed Nevada and the common boundary of California and Nevada. The southwest corner of the map shows the highest frequencies compared to the other corners, indicating the primary pathway of ARs that reached UCRB was the coast of California and the SN. In fact, the majority of valid UCRB ARs were also valid AR events for the SN. According to our identification, 80.2% of the valid UCRB AR days (window edges are not included) were also valid AR days in the SN (see more details in Section 3.3), and that percentage increases to 84.3% if we apply the same analysis for all the days that were affected by ARs. Therefore, the primary source of UCRB ARs is from the southwest, passing over the SN.

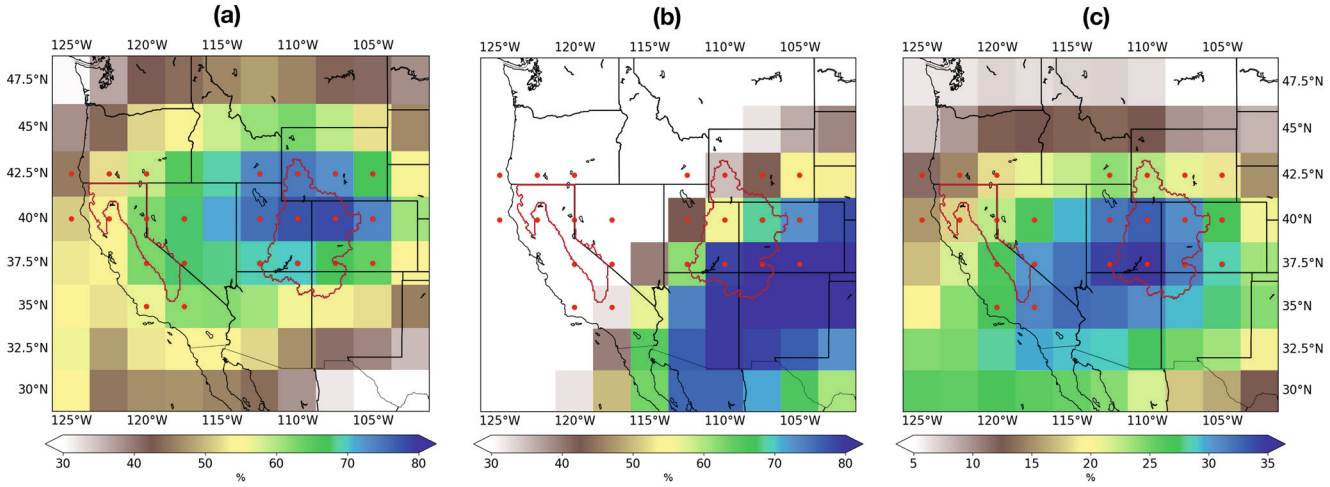

Figure 2. (a) Frequency of valid Upper Colorado River basin (UCRB) atmospheric rivers (ARs) (as described in Section 2.3) for each 2.5° grid cell. (b) The frequency of non-SN UCRB AR occurrence at each 2.5° grid cell. The red dots mark the effective AR region that impacts the UCRB and the Sierra Nevada (SN). (c) Average fraction of AR-snow accumulation (as percentage of the total accumulation induced by ARs) at each 2.5° grid cell.

Other than the ARs that pass through SN, ~15% of UCRB AR days were affected by AR events having different pathways. To examine these AR events (denoted as non-SN UCRB ARs), we excluded the ARs that were valid for both UCRB and the SN and then investigated the occurrences of the remaining ARs over the West. Figure 2b shows the frequency map of non-SN UCRB AR occurrences during the study period. The plot shows that the non-SN ARs in UCRB mainly come from the southwest, first passing over the Gulf of California and Arizona. The pathways of these ARs were further south than the events that first passed over SN. The area that these non-SN ARs most frequently crossed in UCRB is the southeastern part of the domain (dark blue pixels with red dots in Figure 2b). The frequency maps are consistent with the spatial pattern shown in Figure 1a—ARs in UCRB had the greatest impact on snowpack in the Wasatch Range and the least on the northeastern part.

We also calculated fractional snow accumulation for each AR grid cell. The procedure was as follows: given a single valid AR event in UCRB, we first derived the snow accumulation produced by the AR. We then identified all the grid cells in the AR's pathway and assigned the corresponding snow accumulation to those pathway cells. After all the ARs SWE accumulation was assigned, we divided the accumulated SWE at each cell by the total AR-snow accumulation to generate the fractional SWE map as shown in Figure 2c. The high contribution cells demonstrate that ARs are entering the domain from the southwest corner. The grid cells at the highest latitude in the map have the least SWE contribution, indicating the ARs there are passing through from the north without significant impacts on the regions' snow.

3.3. Comparison of AR-Related Snow in UCRB and SN

Because most of the UCRB ARs passed through the SN region, we further explored the AR effects on snow accumulation by comparing the two regions. We calculated the snow accumulation in UCRB associated with non-SN UCRB ARs (i.e., ARs that are only valid in UCRB but not in SN as defined in Section 3.2). On average, the non-SN ARs brought 0.91 km^3 SWE per winter to UCRB, or about 16% of the domain's total AR-related SWE. The mean snowfall in UCRB from all ARs was 4.04 mm/day, which is close to 3.92 mm/day, the average amount of snowfall associated with non-SN ARs (the difference is statistically insignificant at the 0.05 level by the *t* test). Therefore, the pathways of those ARs—whether they come from SN or they enter UCRB via Arizona—does not substantially affect their contribution to UCRB's snowpack.

We applied the same criteria in Section 2.3 to identify valid ARs that intercepted the SN (the 1/16° mask and AR effective region are shown in Figure S4) to explored how the ARs affected snow accumulation. Note that we applied the same 18-h threshold here to extract valid events in the SN because we want to compare the AR's contribution to snow in SN to that in UCRB. Therefore, we need to follow the same approach to

Table 1
Averages of Valid Atmospheric Rivers (AR) Days, AR-Affected Days (Window Edges Included), Accumulated Snow Water Equivalent (SWE), AR-SWE Contribution (as Fraction of Annual Peak SWE), and ΔSWE Accumulation per AR-Affected Day for Dry, Wet, Cold, and Warm Years in Upper Colorado River Basin

	Dry	Wet	Cold	Warm	Climatology
AR days	5.8	14.8	9.8	19.6	11.4
AR-affected days	13.8	31.6	22.0	41.6	26.0
SWE (km^3)	9.6	25.9	28.1	18.8	18.7
AR-SWE contribution	12.9%	40.0%	27.3%	46.4%	29.0%
Avg ΔSWE per AR-affected day (km^3/day)	0.089	0.329	0.348	0.210	0.209

Note. The last column presents the basin-wide climatology over the entire study period.

determine AR-induced SWE from valid ARs in SN. It is not the same as approximating the AR's pathway without any duration threshold. We found that the mean number of valid AR days in the SN was 26.9 days per year over the study period, and 33.8% of those days (9.1 days per year) were also identified as valid ARs in UCRB. Huning et al. (2019) reported that there were on average 22.6–26.5 valid AR days per winter (November 1 to April 1) during 1985–2015 in the SN, which is consistent with our results. The average snowfall in SN associated with ARs was 9.03 mm/day (higher than the average of all snowfall days, 6.52 mm/day), and that number shrinks 31% to 6.25 mm/day if we only consider ARs that failed to reach UCRB (the difference is statistically significant at the 0.05 level by the *t* test). Given these differences in AR-induced snowfall, we conclude that although the pathway of UCRB ARs does not make a large difference to the SWE they deposit in UCRB, the ones intercepted by the SN first yielded great snow accumulation in SN.

3.4. Dry, Wet, Cold, and Warm Years

We selected the 10 most extreme winters in each category (wet, dry, warm, and cold) during the study period and investigated the contributions of ARs in each of these categories to SWE. We defined wet, dry, warm, and cold based on the total precipitation amount or average temperature during the winter season (November 1–March 31) averaged over our domain. Table 1 reports the average number of valid UCRB AR days and AR-snowfall contributions for the four climatic categories and the climatology. Of the four categories, the AR-snow contribution percentage is highest in warm years (46.4%). All the statistics derived from the dry years are the lowest compared to other categories, which illustrates that ARs during dry years are not contributing as much to snow accumulation in the domain as in other years. Although the average snowfall per AR-affected days during cold years are higher than that in warm years, the AR-SWE contribution percentages of cold years (27.3%) are lower than for warm years. AR-related snowfall is higher in the cold years as expected, but the contribution percentage to UCRB's total SWE is less due to greater snow accumulation in the cold conditions. The high amount of SWE (28.1 km^3) and below-average contribution (29.0%) of the cold condition suggest that non-AR-snowfall is more important during these years.

Figure 3 shows bar plots and distribution plots of annual AR-snowfall contributions to UCRB's SWE. The four selected categories (wet, dry, cold, and warm years) are highlighted in the figure. Figure 3b confirms that the AR contribution to UCRB snowpack is higher in wet years and lower in dry years as Table 1 reports. The contributions from cold years tend to be centered near the median as shown in Figure 3d with a below-climatology average (27.3% in the table). Warm years usually have less snow accumulated (18.8 km^3), but AR-SWE contributions from warm years tend to be higher than the climatology, notwithstanding that 2 years occur at the lower end of the distribution. Considering that one of the two low-contribution winters belong to the dry category (the other winter also has below average precipitation), we can conclude that unless the condition is dry, warm years have enhanced AR contributions to snow accumulation.

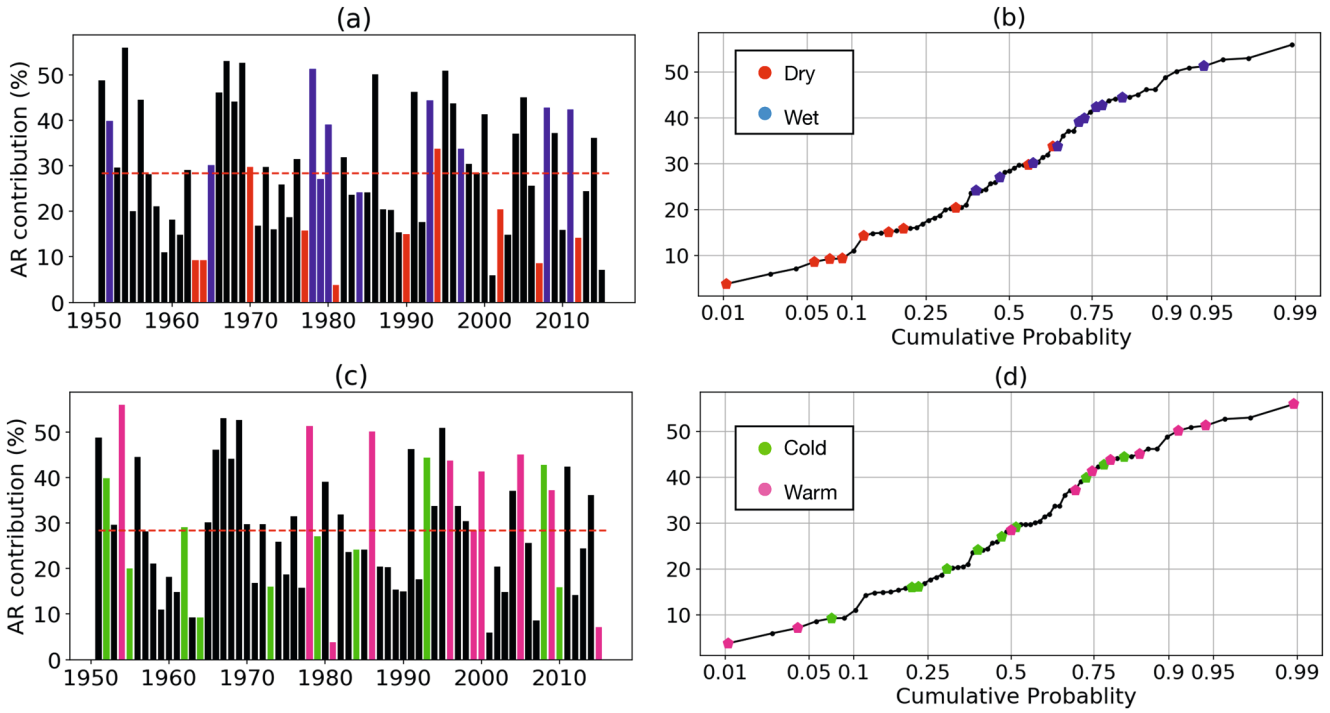

Figure 3. Bar plots (left column) and empirical distributions (right column) of annual atmospheric river-snowfall contribution to peak snow water equivalent (SWE) over the study period. Wet years are highlighted with blue and dry years are with red in panels (a) and (b). Cold years are plotted in green and warm years are in pink in panels (c) and (d).

4. Summary and Conclusions

We applied the VIC model in the UCRB to generate SWE records for winters over 1951–2015. On average, the simulated daily SWE time series successfully captures the major characteristics of SNOTEL observations during the accumulation season (Figure S2). Using the simulated SWE and a long-term reanalysis-based AR catalog from Guan and Waliser (2015), we assessed contributions from ARs to snow accumulation over the UCRB and explored the pathways of these ARs. Specifically, we conclude that:

1. Over the study period, there are on average 11.4 AR-affected days per winter (November–March) in the UCRB, which on average lead to an increase of 5.75 km^3 SWE per winter (30.8% of total winter snow accumulation in UCRB). Compared to the average over all snowfall days, AR-snowfall days are associated with 68% higher snow increase per day (4.04 mm/day versus 2.40 mm/day). The difference is statistically significant at the 0.05 level ($p > 0.05$ by the t test). Calculated on the same basis for the SN region, the AR day snow increase is 9.03 mm/day, which is 38% more than the average 6.52 mm/day for all snowfall days (also statistically significant at the 0.05 level by the t test). In both the SN and UCRB, snow contributions on AR days are greater than ordinary snowfall days, however the enhancement is greater in UCRB than in the SN.
2. The primary origin of UCRB ARs is from the southwest, and most ARs that reach the UCRB intercept the SN first (80.2% of valid AR days in UCRB are also valid AR days in SN). The much smaller remaining number of ARs mostly come from farther south passing over the Gulf of California and Arizona before they reach the UCRB, yielding snowfall primarily in the study domain's southeastern part. The UCRB ARs that do not first cross the SN region yield 3.9 mm/day snowfall during the affected days, which is close to the overall AR-snow contribution for UCRB, 4.0 mm/day (the difference is insignificant at the 0.05 level by the t test). This suggests that the trajectory of ARs that reach the UCRB does not much affect the snowfall magnitude in the UCRB.
3. Only 33.8% of valid AR days (window edges are not included) in the SN are also valid AR days in the UCRB. However, ARs that reach the SN but fail to reach UCRB generally are smaller contributors to SN snowpack than are those that reach UCRB, with average SN snowfall of 6.25 mm per day for ARs that

do not reach UCRB, versus 9.03 mm/day for those that do (statistically significant at the 0.05 level by the *t* test). Although the magnitudes of the ARs that reach UCRB do not appear to be affected by their interception of SN first, those ARs that disappear before reaching UCRB usually yield less SWE in SN.

4. Of all the four climatic categories we selected (wet, dry, warm, and cold years), the AR-snow contribution is highest in warm years (46.4%) and lowest in dry years (12.9%). The amount of AR-related snowfall is also small during dry years. Cold years having larger amounts of AR-snowfall compared to all-year averages as expected, but the contribution to total SWE in these cold years is lower, suggesting that non-AR-snowfall plays a greater role during the cold conditions.

Data Availability Statement

The data used in this study is archived at https://doi.org/10.6084/m9.figshare.14544498.

Acknowledgments
Support for this work was provided in part by Grant No. NA17OAR4310146 from NOAA's Modeling, Analysis, Predictions, and Projections Program to the University of California, Los Angeles, and by the Center for Western Weather and Water Extremes (CW3E) at the Scripps Institution of Oceanography UC San Diego via subcontract to UCLA. We thank Dr. Laurie Huning (California State University, Long Beach) for assistance in accessing the AR catalog used in this study.

References

Albano, C. M., Dettinger, M. D., & Harpold, A. A. (2020). Patterns and drivers of atmospheric river precipitation and hydrologic impacts across the western United States. *Journal of Hydrometeorology*, *21*(1), 143–159. https://doi.org/10.1175/JHM-D-19-0119.1

Andreadis, K. M., Storck, P., & Lettenmaier, D. P. (2009). Modeling snow accumulation and ablation processes in forested environments. *Water Resources Research*, *45*, W05429. https://doi.org/10.1029/2008WR007042

Bohn, T. J., Livneh, B., Oyler, J. W., Running, S. W., Nijssen, B., & Lettenmaier, D. P. (2013). Global evaluation of MTCLIM and related algorithms for forcing of ecological and hydrological models. *Agricultural and Forest Meteorology*, *176*, 38–49. https://doi.org/10.1016/j.agrformet.2013.03.003

Cohen, M., Christian-Smith, J., & Berggren, J. (2013). *Water to supply the land: Irrigated agriculture in the Colorado River basin*. Pacific Institute. Retrieved from http://water.usgs.gov/watercensus/colorado.html

Deems, J. S., Painter, T. H., Barsugli, J. J., Belnap, J., & Udall, B. (2013). Combined impacts of current and future dust deposition and regional warming on Colorado River Basin snow dynamics and hydrology. *Hydrology and Earth System Sciences*, *17*(11), 4401–4413. https://doi.org/10.5194/hess-17-4401-2013

Dettinger, M. (2016). Historical and future relations between large storms and droughts in California. *San Francisco Estuary and Watershed Science*, *14*(2). https://doi.org/10.15447/sfews.2016v14iss2art1

Eldardiry, H., Mahmood, A., Chen, X., Hossain, F., Nijssen, B., & Lettenmaier, D. P. (2019). Atmospheric river-induced precipitation and snowpack during the western United States cold season. *Journal of Hydrometeorology*, *20*(4), 613–630. https://doi.org/10.1175/jhm-d-18-0228.1

Guan, B., & Waliser, D. E. (2015). Detection of atmospheric rivers: Evaluation and application of an algorithm for global studies. *Journal of Geophysical Research: Atmospheres*, *120*, 12514–12535. https://doi.org/10.1002/2015JD024257

Huning, L. S., Guan, B., Waliser, D. E., & Lettenmaier, D. P. (2019). Sensitivity of seasonal snowfall attribution to atmospheric rivers and their reanalysis-based detection. *Geophysical Research Letters*, *46*, 794–803. https://doi.org/10.1029/2018GL080783

Kalnay, E., Kanamitsu, M., Kistler, R., Collins, W., Deaven, D., Gandin, L., et al. (1996). The NCEP/NCAR 40-year reanalysis project. *Bulletin of the American Meteorological Society*, *77*(3), 437–471. https://doi.org/10.1175/1520-0477(1996)077<0437:TNYRP>2.0.CO;2

Kendall, M. G. (1957). Rank Correlation Methods. *Biometrika*, *44*(1/2), 298. https://doi.org/10.2307/2333282

Kirk, J. P., & Schmidlin, T. W. (2018). Moisture transport associated with large precipitation events in the Upper Colorado River Basin. *International Journal of Climatology*, *38*(14), 5323–5338. https://doi.org/10.1002/joc.5734

Li, D., Lettenmaier, D. P., Margulis, S. A., & Andreadis, K. (2019). The role of rain-on-snow in flooding over the conterminous United States. *Water Resources Research*, *55*, 8492–8513. https://doi.org/10.1029/2019WR024950

Li, D., Wrzesien, M. L., Durand, M., Adam, J., & Lettenmaier, D. P. (2017). How much runoff originates as snow in the western United States, and how will that change in the future? *Geophysical Research Letters*, *44*, 6163–6172. https://doi.org/10.1002/2017GL073551

Liang, X., & Lettenmaier, D. (1994). A simple hydrologically based model of land surface water and energy fluxes for general circulation models. *Journal of Geophysical Research*, *99*, 14415–14428. https://doi.org/10.1029/94JD00483

Livneh, B., Bohn, T. J., Pierce, D. W., Munoz-Arriola, F., Nijssen, B., Vose, R., et al. (2015). A spatially comprehensive, hydrometeorological data set for Mexico, the U.S., and Southern Canada 1950–2013. *Scientific Data*, *2*, 1–12. https://doi.org/10.1038/sdata.2015.42

Mann, H. B. (1945). Nonparametric tests against trend. *Econometrica*, *13*(3), 245. https://doi.org/10.2307/1907187

Mote, P. W., Hamlet, A. F., Clark, M. P., & Lettenmaier, D. P. (2005). Declining mountain snowpack in Western North America. *Bulletin of the American Meteorological Society*, *86*(1), 39–50. https://doi.org/10.1175/BAMS-86-1-39

Mote, P. W., Li, S., Lettenmaier, D. P., Xiao, M., & Engel, R. (2018). Dramatic declines in snowpack in the western US. *Npj Climate and Atmospheric Science*, *1*(1), 2. https://doi.org/10.1038/s41612-018-0012-1

Neiman, P. J., Ralph, F. M., Wick, G. A., Lundquist, J. D., & Dettinger, M. D. (2008). Meteorological characteristics and overland precipitation impacts of atmospheric rivers affecting the West Coast of North America based on eight years of SSM/I satellite observations. *Journal of Hydrometeorology*, *9*(1), 22–47. https://doi.org/10.1175/2007jhm855.1

Painter, T. H., Deems, J. S., Belnap, J., Hamlet, A. F., Landry, C. C., & Udall, B. (2010). Response of Colorado river runoff to dust radiative forcing in snow. *Proceedings of the National Academy of Sciences of the United States of America*, *107*(40), 17125–17130. https://doi.org/10.1073/pnas.0913139107

Ralph, F. M., Rutz, J. J., Cordeira, J. M., Dettinger, M., Anderson, M., Reynolds, D., et al. (2019). A scale to characterize the strength and impacts of atmospheric rivers. *Bulletin of the American Meteorological Society*, *100*(2), 269–289. https://doi.org/10.1175/BAMS-D-18-0023.1

Rutz, J. J., & Steenburgh, W. J. (2012). Quantifying the role of atmospheric rivers in the interior western United States. *Atmospheric Science Letters*, *13*(4), 257–261. https://doi.org/10.1002/asl.392

Shields, C. A., Rutz, J. J., Leung, L. Y., Ralph, F. M., Wehner, M., Kawzenuk, B., et al. (2018). Atmospheric river tracking method intercomparison project (ARTMIP): Project goals and experimental design. *Geoscientific Model Development*, *11*(6), 2455–2474. https://doi.org/10.5194/gmd-11-2455-2018

Su, L., Cao, Q., Xiao, M., Mocko, D. M., Barlage, M., Li, D., et al. (2021). Drought variability over the conterminous United States for the Past Century. *Journal of Hydrometeorology*, *22*, 1153–1168. https://doi.org/10.1175/jhm-d-20-0158.1

Swales, D., Alexander, M., & Hughes, M. (2016). Examining moisture pathways and extreme precipitation in the U.S. Intermountain West using self-organizing maps. *Geophysical Research Letters*, *43*, 1727–1735. https://doi.org/10.1002/2015GL067478